Small-Angle Neutron Scattering Study on Uniaxially Stretched Poly(*N*-isopropylacrylamide)−Clay Nanocomposite Gels

Mitsuhiro Shibayama,*,†,‡ Takeshi Karino,†,‡ Sho Miyazaki,† Satoshi Okabe,† Toru Takehisa,§ and Kazutoshi Haraguchi§

Neutron Science Laboratory, Institute for Solid State Physics, University of Tokyo, Tokai, Ibaraki 319-1106, Japan; CREST, Japan Science and Technology Agency, 4-1-8 Honcho Kawaguchi, Saitama 332-0012, Japan; and Kawamura Institute of Chemical Research, 631 Sakada, Sakura-shi, Chiba 285-0078, Japan

Received September 11, 2005; Revised Manuscript Received October 11, 2005

ABSTRACT: The nanocomposite (NC) gels made of poly(*N*-isopropylacrylamide) (PNIPA) and synthetic clay show extraordinarily high mechanical properties, e.g., high extensibility and high strength at break. The structure and deformation mechanism of the NC gels have been investigated by small-angle neutron scattering (SANS). Two-dimensional SANS intensity patterns were obtained for deformed NC4 gels with the stretching ratio up to 6 times, where 4 denotes the clay concentration being 0.04 mol/L (≈3.05 wt %). A so-called abnormal-butterfly pattern was observed in the low q region, i.e., $q < 0.02$ Å^{-1}, while a normal-butterfly pattern was obtained in the larger q (≥ 0.02 Å^{-1}). Here q is the magnitude of the scattering vector. However, contrast-matched SANS experiments disclosed that the abnormal-butterfly pattern is not originated from cross-link inhomogeneities observed in conventional gels but from oriented-clay platelets by deformation. These results indicate that clay platelets, 300 Å in diameter and 10 Å thick embedded in the PNIPA network, are highly aligned with their surface normal parallel to the stretching direction, and the PNIPA chains are elongated parallel to the stretching direction. It is concluded that the high mechanical properties of NC gels are ascribed to "plane cross-linking" with long PNIPA chains between platelets compared with those of conventional chemical gels having "point cross-linking".

Introduction

Polymer−clay nanocomposites have been gathering much attention due to their advanced physical properties than those of the corresponding polymeric systems, such as mechanical properties, heat resistance, improved transmittance, etc.[1,2] Polymer−clay composites are also expected to play important roles in agriculture because of unique polymer and soil (clay) interaction.[3] For example, addition of poly(ethylene glycol) (PEO) to a clay aqueous solution greatly slows down the gelation of the clay solution. Schmidt and co-workers reported a series of small-angle neutron scattering (SANS) works on the rheology−structure relationship of PEO−clay nanocomposite solutions in a shear field, where the clay was exfoliated to nanoplatelets of the order of 10 Å thickness and 300 Å diameter.[4−6] They showed that the clay platelets were oriented with their surface normal parallel to the flow direction, and a dynamic adsorption−desorption equilibrium was attained in the shear field.

Recently, Haraguchi et al. developed novel polymer−clay nanocomposite gels (hereafter we call NC gel).[7] The gels consist of poly(*N*-isopropylacrylamide) and synthetic clay, Laponite, and water. The NC gels exhibit extraordinarily high mechanical properties, such as high elongations (greater than 10 times), high ultimate strengths (of the order of 100 kPa), high transparency (structural homogeneity), large swelling/deswelling ratios, and high deswelling rates.[8,9] The origin of the high mechanical properties as well as gelation mechanism was investigated in terms of viscosity and turbidity measurements during gelation process and by X-ray diffraction of dried gels.[10] Different from the above-mentioned PEO−clay nanocomposite solutions (transient gels), there are a number of facts suggesting the NC gel being a true gel: (1) no sol fraction, (2) swelling/shrinking capability without weight loss, (3) high extensibility, and (4) complete retraction after stretching even more than 5−10 times.[8] It should be also noted that a simple mixing of PNIPA solutions with clay solutions does not behave like the NC gels but remains in a low viscous solution.[10] Therefore, one should recognize that NC gels are completely different system from polymer−clay solutions.

In the previous paper of this series, we discussed the structure and dynamics of NC gels by SANS and dynamic light scattering (DLS).[11] It is known that clay platelets themselves form a house-of-cards structure in an aqueous solution.[4,12] On the other hand, we observed that clay platelets are strongly tied with each other by polymer chains in a NC gel.[11] However, the origin of the novel mechanical properties has not been elucidated because most studies were carried out for undeformed gels. Hence, structural analyses of NC gels under deformation have been highly desired. In this paper, we report small-angle neutron scattering (SANS) results on deformed NC gels and discuss the deformation mechanism. We employ both contrast-matched SANS in addition to the ordinal SANS. That is, the scattering length density of the solvent was matched to that of clay. This allowed us to investigate only the deformation of PNIPA chains up on stretching.

Experimental Section

Samples. *N*-Isopropylacrylamide (NIPA) monomer (Kohjin Co., Ltd., Japan) was purified by recrystallization from a

† University of Tokyo.
‡ CREST, Japan Science and Technology Agency.
§ Kawamura Institute of Chemical Research.
* To whom correspondence should be addressed. E-mail: sibayama@issp.u-tokyo.ac.jp.

10.1021/ma051979h CCC: $30.25 © 2005 American Chemical Society
Published on Web 11/09/2005

toluene/*n*-hexane mixture, followed by drying in vacuo. As an inorganic clay, synthetic hectorite "Laponite XLG" (Rockwood Ltd.: $[Mg_{5.34}Li_{0.66}Si_8O_{20}(OH)_4]Na_{0.66}$), was used. The purified monomer was dissolved in deionized water (or D_2O) containing dispersion of the inorganic clay. The NIPA monomer concentration was 690 mM (7.8 wt %). Prior to dissolution, oxygen in the deionized water (or D_2O) was removed by bubbling N_2 gas for 2 h. Potassium peroxodisulfate (KPS) and *N*,*N*,*N*′,*N*′-tetramethylethylenediamine (TEMED) were used as an initiator and catalyst, respectively. The molar ratio of the monomer, initiator, and catalyst was 100:0.426:0.735. Redox polymerization was carried out in a Teflon mold of 2 cm wide, 4 cm long, and 4 mm thick at 20 °C for 20 h. Thus, prepared slab gels were set to a stretching device. The sample codes for the clay solutions and gel were defined by the ratio of the clay and water, i.e., Clay4 and NC4, respectively. This indicates 0.04 mol of clay (= 30.48 g) in 1 L of H_2O or D_2O, for both the clay solution and gel. For comparison, a conventional PNIPA gel cross-linked with *N*,*N*′-methylenebis(acrylamide) (BIS) was also prepared. The BIS concentration was 3 mol % with respect to NIPA monomer, and the NIPA concentration was 1 M. Hence, we call this gel OR3. The mass densities of the clay and dry PNIPA were evaluated to be $d_{clay} = 2.65$ g/cm^3 and $d_{NIPA} = 1.26$ g/cm^3 obtained by density measurements.[7]

Small-Angle Neutron Scattering (SANS). SANS experiments were performed at the two-dimensional SANS instrument (SANS-U), Neutron Science Laboratory, the University of Tokyo.[13] The neutron wavelength was 7.0 Å. The monochromatization was attained with a mechanical velocity selector, and the wavelength distribution was ca. 10%. The sample-to-detector distance (SDD) was 2 and 8 m. The scattered neutrons were collected with a two-dimensional detector (model 2660N, Ordela), and then a sector average was taken before necessary corrections, such as air scattering, cell scattering, and incoherent background subtraction.[14] After these corrections, the scattered intensity was normalized to the absolute intensity, i.e., the differential scattering cross section in terms of scattering intensity from a standard sample. The temperature of the samples was regulated to be 20 °C with a water-circulating bath controlled with a Neslab RTE-111 thermocontroller with a precision of ±0.1 °C. The stretching experiment was conducted with the following procedure. The sample was stretched stepwise with the step of $\Delta\lambda = 0.2$ (up to $\lambda = 2.0$), $\lambda = 2.5$, and then $\Delta\lambda = 1.0$ (from $\lambda = 3.0$ up to $\lambda = 6.0$). Here, λ ($\equiv l/l_0$) is the stretching ratio, and l_0 and l are the sample lengths before and after stretching, respectively. After every stretching step, 10 min was allowed for structural equilibration. The SANS measuring time was 10 min for the case of SDD = 2 m and 2 h for SDD = 8 m. The humidity of the sample environment was kept constant by placing a bottle of water near the sample in a shielded-stretching chamber throughout the experiment. The weight loss of the sample in the chamber was measured to be about 7% for 20 h. We believed that this was within the allowance for the investigation of the structural change of NC gels by deformation.

Results and Discussion

1. Mechanical Properties. Figure 1 shows the stress−strain curves of NC4 and OR3. The tensile modulus of OR3 is higher than NC4. It is obvious that the relative magnitudes of the tensile moduli of OR and NC gels depend on the cross-linker concentration as studied by Haraguchi et al.[8,9] However, it is noteworthy that the ultimate mechanical properties of NC4 are much superior to those of OR3, e.g., the strength at break being 87.8 kPa (ca. 10 times as high as that of OR3, 9.4 kPa) and the maximum strain (= $(\lambda - 1)_{NC}$) being 1040% (ca. 50 times as high as that of OR3, 21%). Although some stress-relaxation behavior was observed at large deformation (e.g., $\lambda > 4$), such a large deformability without breaking is one of the unique properties of NC gels.[7] Note that the stress-relaxation behavior itself is completely recovered by aging without strain.

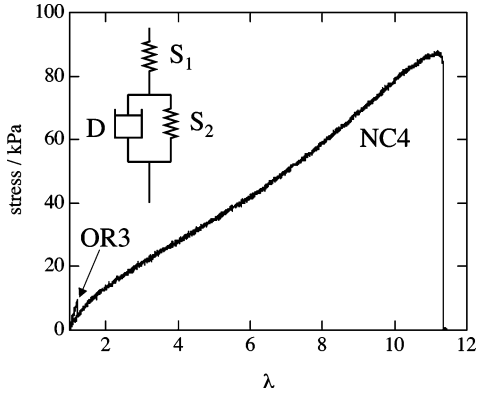

Figure 1. Stress−strain curve of NC4 (nanocomposite gel cross-linked with clay) and OR3 (conventional chemical gel cross-linked with BIS). The inset shows the mechanical model for the NC gels with springs S_1 and S_2 and a dashpot D.

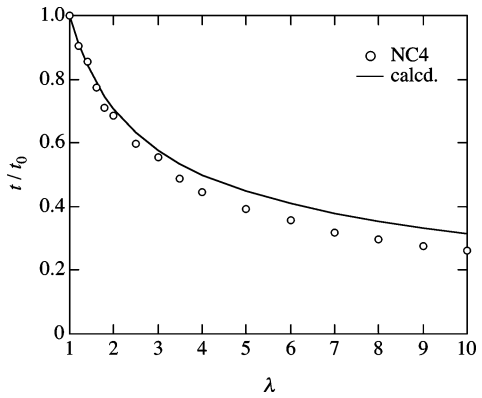

Figure 2. Stretching ratio dependence of the sample thickness. The solid line was obtained by assuming rubberlike deformation.

Thus, the deformation mechanism of NC4 can be represented by a three-component mechanical model shown in the inset of Figure 1. That is, the model is a series of a spring (S_1) and a Voigt model consisting of another spring (S_2) and a dashpot (D).

Figure 2 shows the variation of the normalized sample thickness, t/t_0, as a function of the stretching ratio, λ, subject to a uniaxial stretching, where t_0 and t are the sample thicknesses before and after stretching, respectively. The solid line denotes a theoretical curve obtained with an assumption of a constant-volume deformation, i.e.

$$t = \frac{t_0}{\sqrt{\lambda}} \tag{1}$$

To ensure the reproducibility of the measurement, about 10 min was awaited before thickness measurement whenever the sample was stretched, and the thickness was measured three times and an average was taken. As shown in the figure, a constant-volume deformation took place up to $\lambda \approx 2$, and a negative deviation occurred at higher elongation. This is due to stress-relaxation of the sample at high elongations. However, after releasing the strain, the sample recovered its original length even for the case of $\lambda = 6.0$ if the sample was stretched and released quickly. On the other hand, a considerable stress-relaxation behavior was observed for stretched NC4 after completion of a series of SANS measurement by spending 1 day. Hence, it is concluded that NC gels exhibit a rubberlike deformation behavior for instant

stretching/releasing, while a viscoelastic deformation behavior subject to a standing load. Interestingly enough, the sample recovers its original length by aging at room temperature for a considerable time, e.g., half a day. All of these experimental findings support the mechanical model proposed in the inset of Figure 1.

2. SANS. 2.1. Clay Scattering and Contrast Matching. In the case of a three-component system consisting of PNIPA, clay, and solvent, the scattering intensity function can be obtained by[15]

$$I(q) = \phi_P\phi_S(\rho_P - \rho_S)^2 S_{PP} + \phi_C\phi_S(\rho_C - \rho_S)^2 S_{CC} + 2\phi_P\phi_C(\rho_P - \rho_S)(\rho_C - \rho_S)S_{PC} \quad (2)$$

where ϕ_i and ρ_i are the volume fraction and the scattering length density of the component i (= P, C, and S). Here, P, C, and S denote the polymer (PNIPA), clay, and the solvent, respectively. $S_{PP}(q)$, $S_{CC}(q)$, and $S_{PC}(q)$ are the polymer−polymer, clay−clay, and polymer−clay structure factors, respectively. If one tunes ρ_S to be equal to ρ_C, eq 2 becomes

$$I(q) = \phi_P\phi_S(\rho_P - \rho_S)^2 S_{PP} \quad (3)$$

Hence, the scattering from clay disappears, and only the information from the polymer chains can be evaluated. This is the so-called contrast-matching.

Prior to the contrast-matched SANS experiment of NC gels, we evaluated the contrast-matching point for clay in water. The scattering length densities of the clay and PNIPA were calculated to be $\rho_{clay} = 3.92 \times 10^{10}$ cm^{-2} and $\rho_{NIPA} = 0.933 \times 10^{10}$ cm^{-2} by using the mass densities of clay and PNIPA, respectively. Figure 3 shows the SANS intensity curves, $I(q)$s, for Clay4 in water with various D_2O compositions. Here, the D_2O fraction, f_{D_2O}, was systematically varied from 0 to 100 vol % D_2O. As shown in the figure, $I(q)$s look superimposable with each other and have the lowest scattering at around $f_{D_2O} = 66\%$. The structure factor, $S_{CC}(q)$, can be calculated as the scattering function for randomly oriented thin platelets, i.e.

$$S_{CC}(q) = V\int_0^{\pi/2}\left\{\frac{2J_1(qR\sin\alpha)}{qR\sin\alpha}\frac{\sin(qH\cos\alpha)}{qH\cos\alpha}\right\}^2 \sin\alpha\, d\alpha \approx V\int_0^{\pi/2}\left\{\frac{2J_1(qR\sin\alpha)}{qR\sin\alpha}\right\}^2 \sin\alpha\, d\alpha \quad (4)$$

where $2H$ and R are the thickness and the radius of the platelet, respectively, and α is the polar angle with respect to the direction along the platelet normal. V is the volume of a clay platelet, i.e., $V = 2\pi R^2 H$. $J_1(x)$ is the Bessel function of the order of 1. The solid lines are calculated scattering function with the literature values for the clay, i.e., $2R = 300$ Å and $2H = 10$ Å.[11,12] As shown in the figure, the observed SANS functions are well reproduced with eq 4. The deviations at low q's may result from destructive interference between platelets, which gives rise to a broad peak at $q_m \approx 0.015$ Å^{-1}. Hence, the interparticle spacing can be estimated to be $2\pi/q_m \approx 400$ Å.[4,12]

Figure 4 shows the variation of $I(0)$ for Clay4 with the solvent composition. Here, $I(0)$s were obtained by extrapolating the observed scattering functions in Figure 3 to $q = 0$ with eq 4. As shown in the figure, the

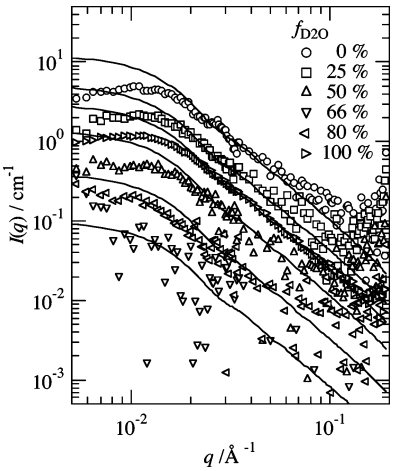

Figure 3. Scattering functions of Clay4 in waters having various scattering length densities. The solid lines are calculated curves with eq 4.

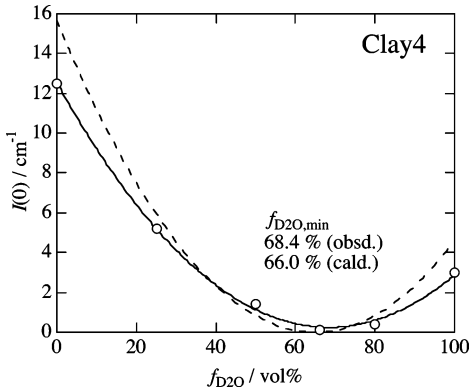

Figure 4. D_2O fraction dependence of the $I(0)$s for Clay4: observed (solid line) and calculated (dashed line).

observed values for $I(0)$s well fit to the parabolic function with f_{D_2O} (the solid curve). The minimum is evaluated to be $f_{D_2O} = 68.4\%$. Note that $I(0)$ is calculated by the following equation

$$I(0) = \phi_C\phi_S\{\rho_C - \rho_S(f_{D_2O})\}^2 S_{CC}(0) \approx \phi_C\{\rho_C - \rho_S(f_{D_2O})\}^2 V \quad (5)$$

where $\rho_S(f_{D_2O})$ is the scattering length density of the solvent with f_{D_2O}. Thus, calculated function has a minimum at $f_{D_2O} \approx 66\%$ as shown by the dashed line in Figure 4, which is in good agreement with the observed one. Therefore, a contrast matching was attained with $f_{D_2O} \approx 66\%$. This result also agrees well with the one reported by Lal for poly(ethylene glycol)−clay mixture in water.[15]

On the basis of this estimation, we chose two experimental conditions to be (A) a off-matched case with D_2O ($\rho_{D_2O} = 6.35 \times 10^{10}$ cm^{-2}) as a solvent and (B) the contrast-matched case with a $f_{D_2O} \approx 66\%$. The experimental conditions of case A and case B provide information on the overall scattering, i.e., $S_{PP}(q)$, $S_{CC}(q)$, and $S_{PC}(q)$ (case A) and only on the PNIPA chain scattering, $S_{PP}(q)$ (case B).

2.2. Off-Matched Scattering: Case A. Figure 5 shows a series of two-dimensional scattering patterns obtained for uniaxially deformed NC4 in D_2O ($f_{D_2O} = 100\%$). The stretching ratios are $\lambda = 1.0$, 2.0, 4.0, and 6.0. The upper and lower columns show SANS patterns

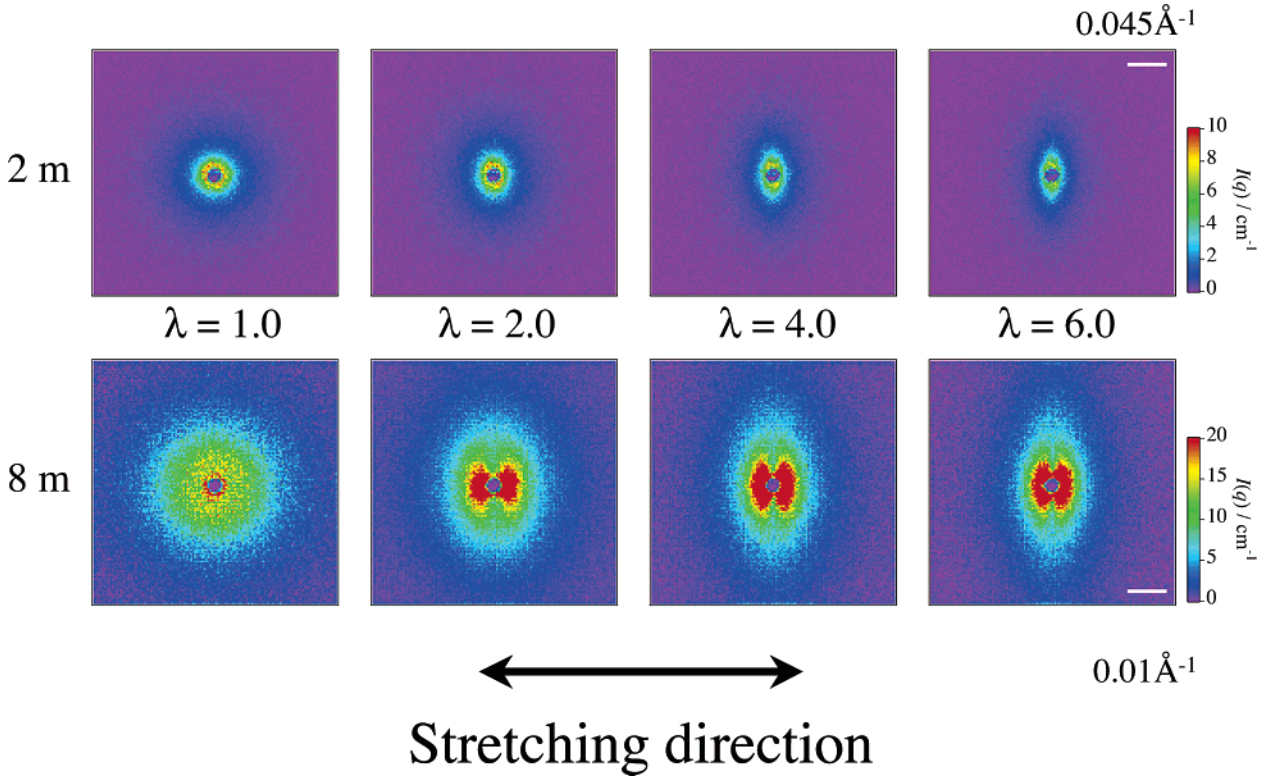

Figure 5. Two-dimensional SANS patterns for NC4 in D_2O (case A): upper (SDD = 2 m) and lower (SDD = 8 m).

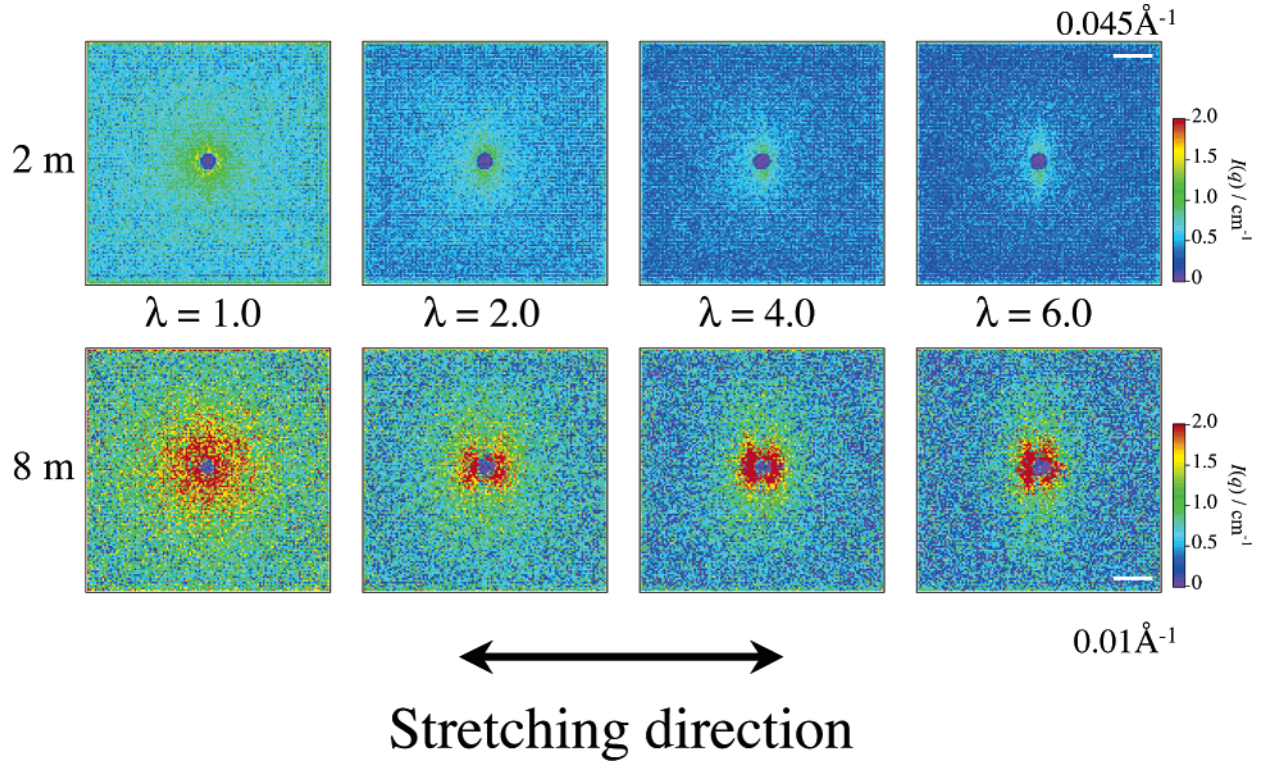

Figure 6. Two-dimensional SANS patterns for NC4 in a contrast-matched solvent (case B): upper (SDD = 2 m) and lower (SDD = 8 m).

taken with SDD = 2 and 8 m, respectively. The stretching direction was horizontal. As shown here, the 2 m scattering patterns became elliptic with their long axis oriented perpendicular to the stretching direction. On the other hand, the 8 m scattering patterns clearly show that there is another component showing a two-lobe pattern strongly oriented in the stretching direction (in red) in addition to the perpendicularly oriented elliptic pattern (in green). To elucidate the origin of these scattering, we carried out a contrast-matched SANS experiment.

2.3. Contrast-Matched Scattering: Case B. Figure 6 shows a series of two-dimensional scattering patterns obtained for uniaxially deformed NC4 in the contrast-matched solvent with f_{D_2O} = 66%. In this case, the structure information about PNIPA chains is exclusively

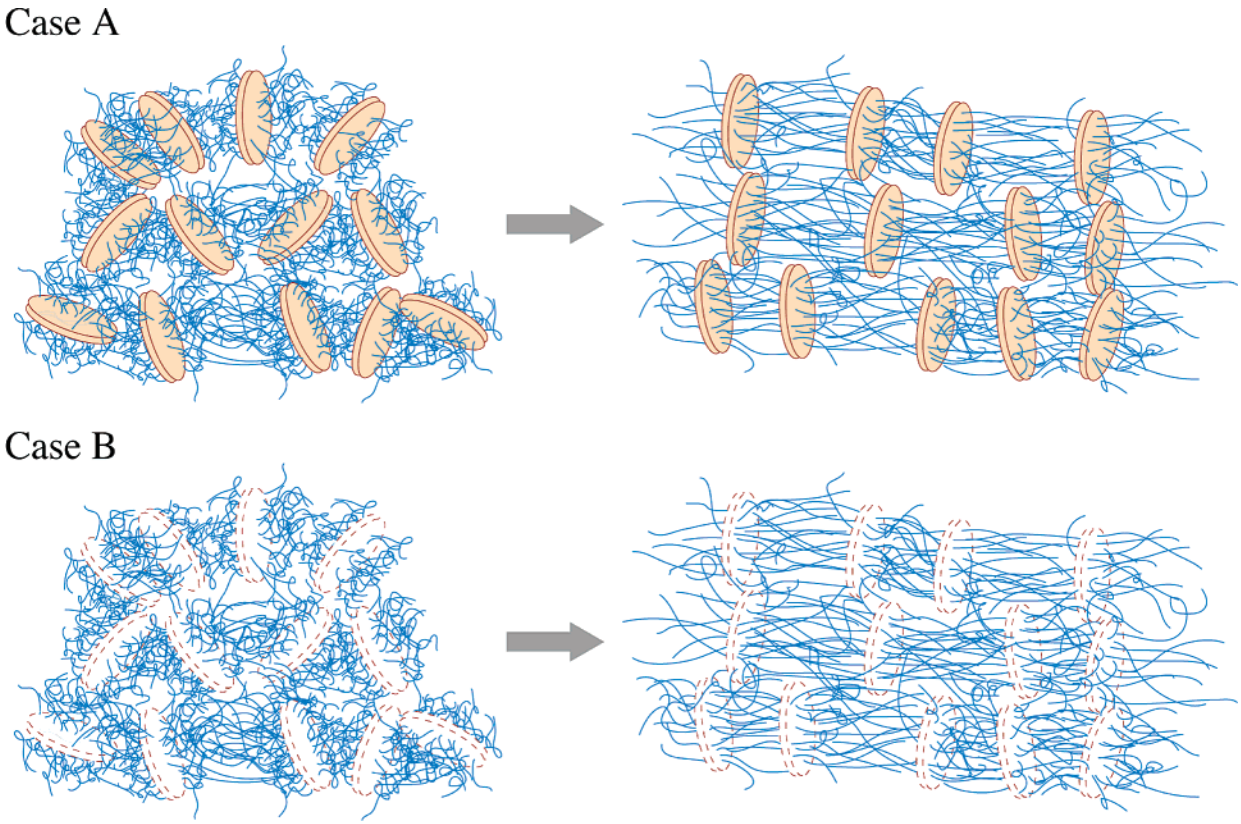

Figure 7. Schematic representation of NC gels before (left) and after stretching (right): case A (in D_2O) and case B (in a contrast-matched solvent).

obtained. Interestingly, a two-lobe pattern localized in the stretching direction is also observed in the 8 m scattering pattern. This pattern is similar to those observed in chemically cross-linked gels called the "abnormal-butterfly pattern".[16−18] The abnormal-butterfly patterns observed in chemical gels are ascribed to an increase in inhomogeneities due to nonrandom cross-linking in gels that become explicit by deformation.[19,20] In addition, Schmidt and co-workers[4−6,21] observed abnormal butterfly patterns in PEO−clay nanocomposite solutions. The clay platelets are oriented with their surface normal perpendicular to the flow direction (or parallel to the shear direction), and an abnormal pattern appeared in the shear direction. Hence, we are tempted to conclude that NC gels also possess cross-linking inhomogeneities similar to those of chemically cross-linked gels and to polymer−clay nanocomposite solution in a flow field. However, as will be discussed later, the "abnormal-butterfly pattern" observed in NC gels is related to clay orientation. Note that the patterns in Figure 6 are very different form those observed in the slide-ring (SR) gels as recently reported by Karino et al.[22] The SR gels have movable cross-links made of cyclodextrin, which minimize the strain generated in the gel by deformation. Because of these unique properties, an analogy may hold between the polymer chains in a stretched SR gel and polymer chains in a flow field. As a result, SR gels exhibit a normal butterfly pattern by uniaxial deformation.

Figure 7 shows a schematic illustration of undeformed (left) and stretched NC gels (right). The upper is case A where both the clay platelets and PNIPA chains are "visible", while only PNIPA chains are visible in the lower (case B). In the undeformed state, clay platelets are randomly oriented, to which PNIPA chains are ancohred. By stretching the gel, on the other hand, clay platelets become oriented perpendicular to the stretching direction, giving rise to a strong scattering along the stretching direction. It is important to note that an "abnormal-butterfly pattern" is also seen in the contrast-matched sample (see Figure 6). Now, let us focus on the conformation changes of PNIPA chains by deformation.

2.4. Analysis of the Anisotropy. The scattering function, $I(q)$, of deformed gels can be separated to (i) a scattering function from clay platelets and (ii) that from deformed polymer chains. The polymer chain deformation can be evaluated from the contrast-matched SANS data taken with SDD = 8 m. Figure 8 shows sector-averaged scattering intensities, $I_{para}(q)$ and $I_{perp}(q)$, as a function of q for the SANS intensity curves in Figure 6 in the parallel and perpendicular directions, respectively. Here, the sector average was taken with the sector angle of 10°. Though the data are highly scattered because of the lack of counting statistics, both $I_{para}(q)$ and $I_{perp}(q)$ are monotonic functions of q.

Figure 9 shows the so-called Ornstein−Zernike (OZ) plots, i.e., $I_{para}^{-1}(q)$ and $I_{perp}^{-1}(q)$ vs q^2.

$$\frac{1}{I_{para}(q)} = \frac{1 + \xi_{para}^{2} q_{para}^{2}}{I_{para}(0)}, \quad \frac{1}{I_{perp}(q)} = \frac{1 + \xi_{perp}^{2} q_{perp}^{2}}{I_{perp}(0)} \tag{6}$$

Here, ξ_{para} and ξ_{perp} are the correlation lengths of the PNIPA chains in the parallel and perpendicular directions, respectively. At $\lambda = 1.0$, both $I_{para}(q)$ and $I_{perp}(q)$ were identical as they should be. However, at $\lambda = 2.0$, a significant difference between $I_{para}(q)$ and $I_{perp}(q)$ was observed. By curve fitting the experimental data with eq 6, the correlation lengths and the zero-q intensities were evaluated. It should be noted here that the scattering intensity is well represented by an OZ

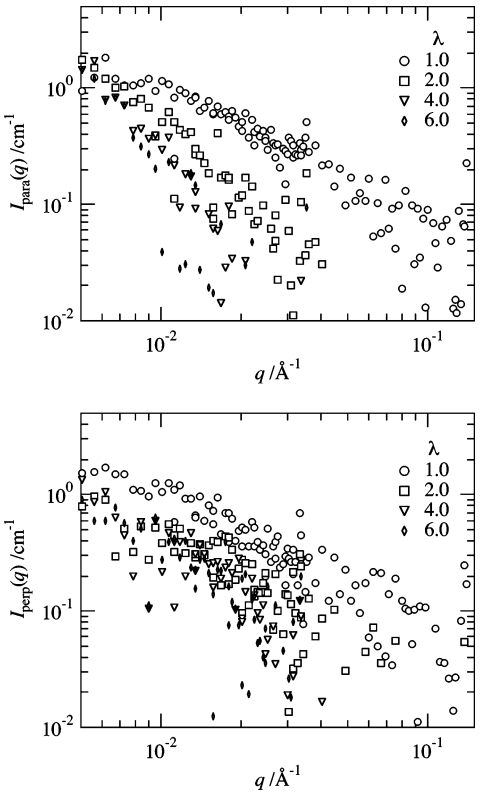

Figure 8. Sector-averaged SANS intensity functions, $I_{para}(q)$ and $I_{perp}(q)$, with various stretching ratios.

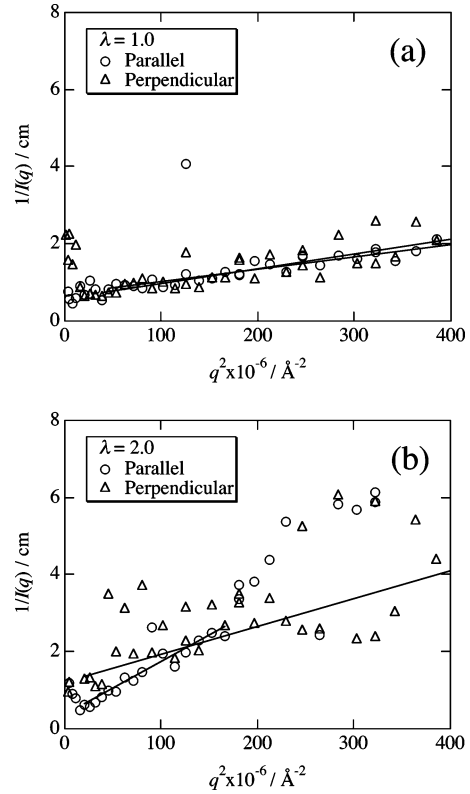

Figure 9. OZ plots of (a) undeformed and (b) deformed NC4.

function. In general, polymer gels possess cross-linking inhomogeneities, which are observed as a squared-Lorentz function.[23] The absence of the squared-Lorentz term means that no significant cross-link inhomogeneities exist in the NC gel. In the previous paper, we concluded that NC gels have cross-link inhomogeneities.[11] However, it should be corrected to the following

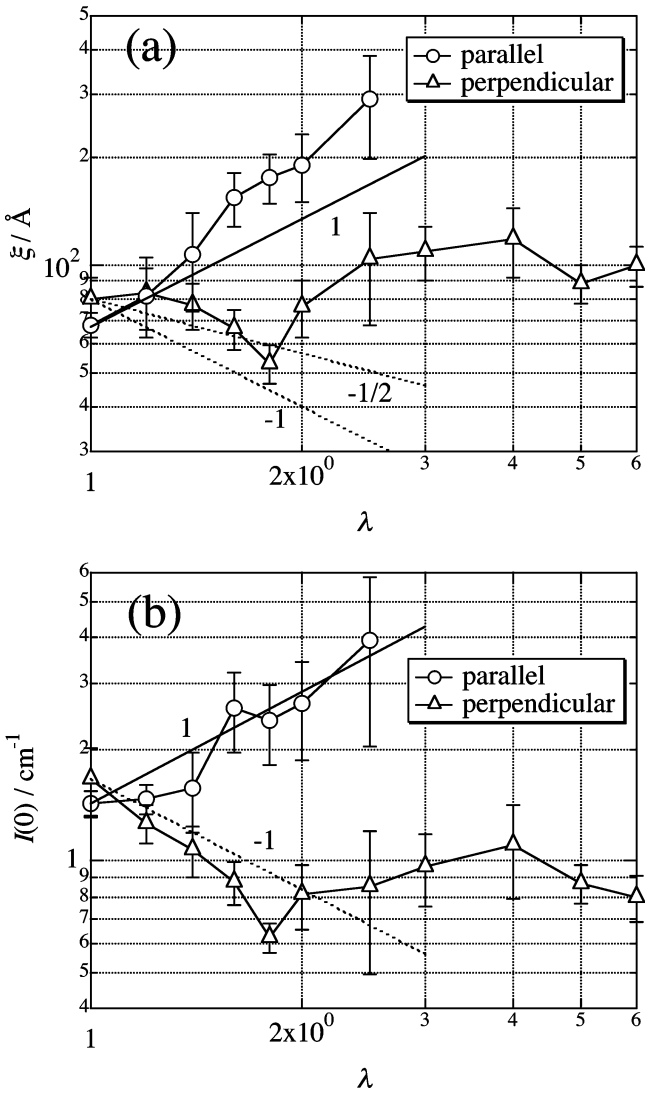

Figure 10. Variations of (a) the correlation lengths and (b) the zero-q intensities. The solid and dashed lines indicate power laws with the numbers given in the figure. The error bars are also shown.

statement. That is, these inhomogeneities are mainly due to the clay−clay, $S_{CC}(q)$, and the clay−polymer scatterings, $S_{CP}(q)$.

The variations of ξ_{para} and ξ_{perp} are plotted with error bars in Figure 10a as a function of λ in a double-logarithmic plot. At $\lambda = 1.0$ both values are almost identical. The correlation length, ξ_0, for the undeformed state is evaluated to be $\xi_0 \approx \xi_{para} \approx \xi_{perp} \approx 70$ Å, which is much larger than the typical value of chemically cross-linked gels at the same polymer concentraion, i.e., $\xi_0 \approx 20$ Å.[24] This correlation length may be related to a "blob" separated by neighboring clay platelets. Even though the clay scattering is erased by contrast matching, the space occupied by a clay platelet is substituted by the water having the same scattering length density. Hence, although the polymer−polymer correlation is "invisible", the blob scattering characterized by ξ_{para}, and ξ_{perp} is detected due to the presence of "shadow" of the clay platelets. With increasing λ, the difference between ξ_{para} and ξ_{perp} increases, indicating that the anisotropy becomes large. As shown by the solid line, ξ_{para} increased rather linearly with λ. On the other hand, the λ dependence of ξ_{perp} exhibited an interesting behavior and had a kink around $\lambda = 2$. In view of the error bars,

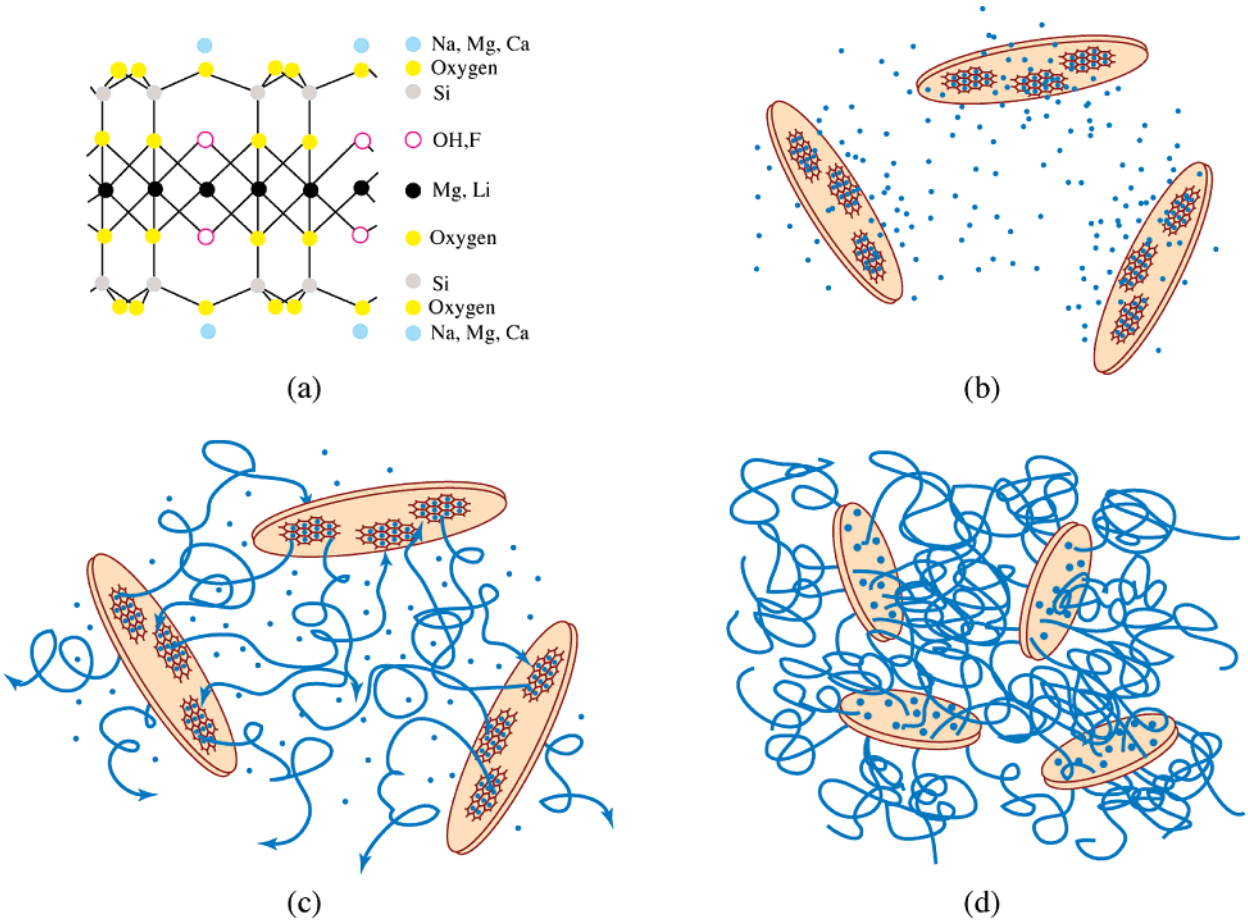

Figure 11. Schematic representation of the structure of NC gels. (a) The chemical structure of clay platelet. (b) to (d) show the structure of NC gels (b) before polymerization of NIPA, (c) during polymerization, and (d) after polymerization. The brown disks, blue dots, and blue lines indicate clay platelets, NIPA monomers, and PNIPA chains, respectively.

the kink and curvature are larger than the statistical errors. Hence, we conjecture that these kink and curvature are related to a rotation of clay platelets by stretching. That is, clay rotation leads to rearrangement of PNIPA chains. Since the interplatelet distance (≈400 Å^{-1}) is not large enough compared to the diameter of the platelet (≈300 Å^{-1}), the interplatelet distance has to increase to make space for platelet rotation. After rotation, the distance becomes shorter. If one neglects this kink, on the other hand, it is concluded that ξ_{perp} decreased gradually with λ up to $\lambda = 2.0$, which also obeys more or less the predicted variation with the assumption of affine deformation, i.e., $\xi_{perp} \sim \lambda^{-1/2}$ (indicated the dashed line). The increase of ξ_{para} indicates an increase in the interplatelet distance (or elongated blobs) and the decrease of ξ_{perp} does to squeezed blobs. In the region where $\lambda \geq 2.0$, ξ_{perp} further increased with increasing λ, suggesting the presence of highly stretched blobs. On the other hand, ξ_{perp} leveled off around $\xi_{perp} \approx 100$ Å for $\lambda \geq 2.0$. This may be related to the stress-relaxation behavior observed in the mechanical measurement. However, it is difficult to discuss in more detail because of the poor statistics in the SANS data.

Figure 10b shows that a similar behavior to Figure 10a is found also in the variations of $I_{para}(0)$ and $I_{perp}(0)$. $I_{para}(0)$ increases at low q regions, and $I_{perp}(0)$ decreases with increasing λ. It is very important to note that no "abnormal" behavior is observed in the λ dependence of $I_{para}(0)$ and $I_{perp}(0)$ even in the case of the contrast-matched SANS (case B). The increase in $I_{para}(0)$ is simply due to an increase in ξ_{para}. The observed "abnormal-butterfly pattern" is ascribed to an orientation of clay platelets by stretching because the scattering is observed as a "shadow" even in the case of the contrast-matched gel. This argument readily leads to an important statement that "the NC gels have very low cross-link inhomogeneities". This is why no increase in cross-link inhomogeneities appears by deformation. The question of high transparency in NC gels addressed in the Introduction can be answered with the same reason. That is, the cross-link inhomogeneities in NC gels are much lower than chemically cross-linked polymer gels because of the absence of chemical cross-links inhomogeneously introduced during polymerization.

3. Structure of NC Gels and Deformation Mechanism. On the basis of the experimental findings disclosed in the previous section, we discuss the structure and deformation mechanism of NC gels. A clay platelet itself consists of a sheetlike structure with various kinds of atoms, as shown in Figure 11a. The oxygen atoms on the clay surface may be capable of hydrogen bonding with the amide proton of NIPA, and the metal ion of the clay surface may form a complex with the carbonyl oxygen of NIPA. If such a hydrogen bonding is formed, NIPA monomers are strongly bound to the clay surface. Hence, by addition of NIPA monomer into a clay solution, a house-of-cards structure is broken and the solution viscosity decreases.[8,10] When polymerization of NIPA is initiated by radical species, PNIPA chain grows by anchoring one end to the surface of a clay as shown in Figure 11b,c, while many of NIPA

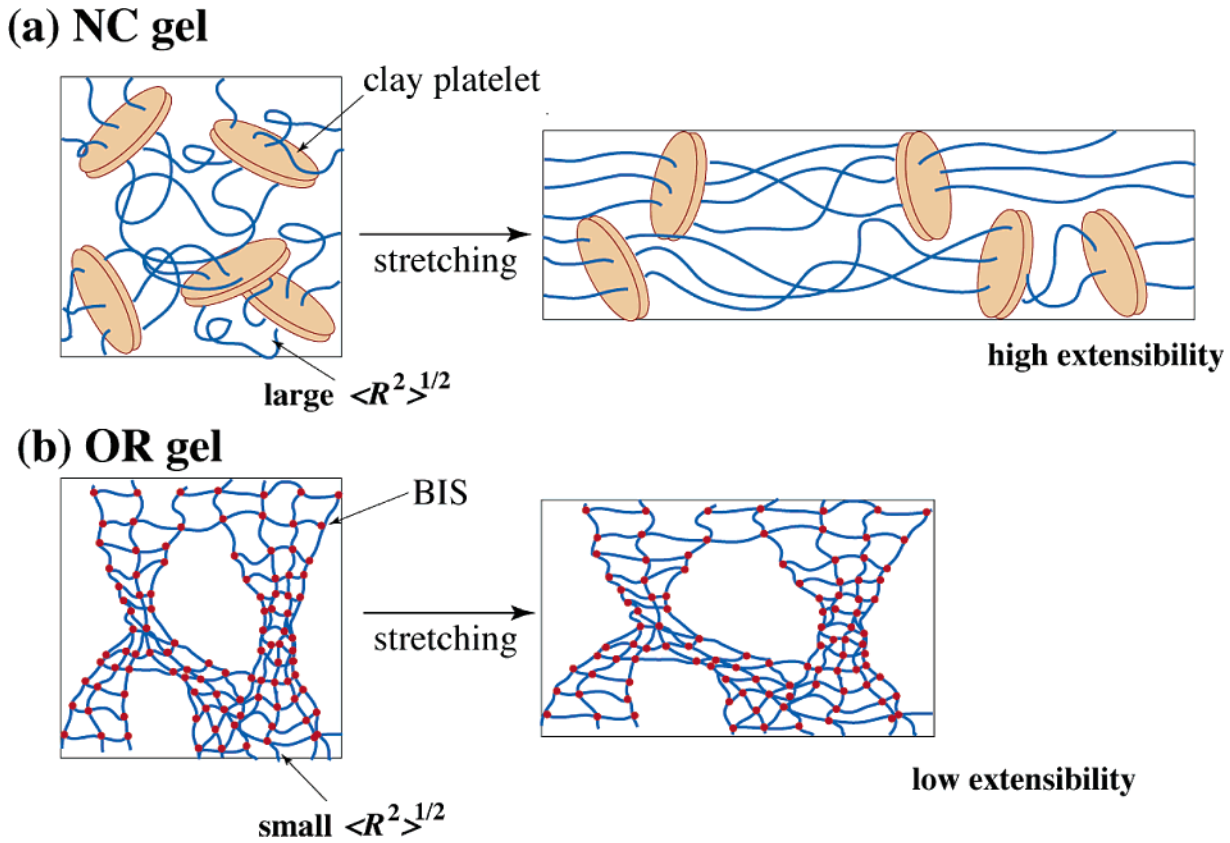

Figure 12. Deformation model of (a) NC gels and (b) OR gels. PNIPA chains in NC gels are effectively bridging clay platelets, and the molecular weight is rather high compared with those of OR gels.

monomers remain unreacted. The propagation of PNIPA chains may terminate by hitting another monomer on a platelet or by encountering quenching species, such as oxygen. The former leads to a formation of a bridging chain between neighboring clay platelets, and the latter results in a dangling-chain formation. As a result, PNIPA gels cross-linked with clay platelets are formed as schematically depicted in Figure 11d. This model is supported by the finding by Haraguchi et al.[10] They studied wide-angle diffraction patterns of a series of dimethylacrylamide (DMAA) nanocomposite gel D-NC2.5 in the dried state and observed that the Bragg spacing changed systematically with DMAA content. The interplatelet distance, L, was a linear function of the DMAA concentration in M, m [M], as follows:

$$L\ [\text{Å}] = 13\ [\text{Å}] + km\ [\text{M}] \qquad (7)$$

where k is a constant and $k = 59.4$ [Å/M]. This linear relationship indicates that (1) the clay platelet distance in the absence of PNIPA chains, i.e., the platelet thickness, is 13 Å and (2) the clay platelets are aligned in a one-dimensional array at least locally and PDMAA chains are intercalated between the platelets. Since the area of platelets is invariant (300 Å in diameter), an increase in the PDMAA content simply results in an increase in the interplatelet distance in a linear fashion. If considerable amount of PDMAA chains are not bound to platelets, the above relation does not hold. The same argument is applicable to PNIPA−clay gels (i.e., NC4). It should be stressed here that because of initial adsorption of NIPA monomers on a clay platelet the ratio of the bridge formation is very high compared with dangling or loop chain formation. This is one of the origins of the good mechanical properties of NC gels. Therefore, the structure of NC gels is very different from that of conventional chemical gels. Now we discuss the essential difference between the two types of gels.

Figure 12 shows the difference in the structure of NC gels and OR gels. First of all, the "spatial" inter-cross-link distance of a NC gel; i.e., the interplatelet distance is much longer (of the order of 400 Å) than the inter-cross-link distance of OR gels (of the order of 10−20 Å for the case of 700 mM PNIPA gels with 5% cross-links).[24,25] Second, the "topological" chain lengths $\langle R^2\rangle^{1/2}$ are also very different, where R is the end-to-end distance of PNIPA chains between cross-links and $\langle\ \rangle$ denotes ensemble averaging. That is, the molecular weight of PNIPA chains bridging neighboring clay platelets is much larger than that of subchains between cross-links for OR gels. The former could be of the order of 10^5−10^6 Da,[26] while the latter is of the order of 10^1−10^2 Da (based on the ratio of NIPA and BIS). Third, the number of "effective" cross-links, which are capable of transmitting the external load, is much larger in NC gels than in OR gels. This is because most of PNIPA chains in NC gels are anchored to clay platelets and play a role as active chains, while most of PNIPA chains in OR gels are separated by cross-linkers to short chains and merely form clusters with a high density of cross-linking. These facts directly result in the high elongation ratio and high strength at break of NC gels. Upon stretching, clay platelets become oriented with their surface normal parallel to the stretching direction.

The clay orientation in NC gels by stretching is quite different from that of PEO−clay solutions, where clay platelets are oriented with their surface normal perpendicular to the flow direction. It should be noted here that there seem to be two cases of the clay orientation

for polymer−clay solutions in a flow field. One is the case that clay platelets are oriented with their normal parallel to the vorticity direction (laponite; the same clay as employed in this work).[4,21] The other is the case where clay platelets are oriented with their normal parallel to the velocity direction (CNA, cloisite with 700−1500 Å diameter and 10 Å thickness).[27] Hence, apart from the fact that the clay platelets are aligned with their normal perpendicular to the flow direction, the orientation of clay platelets seems to be still controversial or dependent on the system. The bottom line is, however, that the polymer chains are commonly oriented in the stretching (NC gel) and in the flow directions (polymer−clay solutions). The essential difference between the two cases is whether or not the polymer chains bear an external stress. In the case of NC gels, the PNIPA chains bear an external stress and are highly deformed to sustain the load. Since the chains are anchored to clay platelets, the chains have to be perpendicularly oriented with respect to the clay surface in order to transmit the external force. On the other hand, clay platelets in a flow field orient so as to reduce the hydrodynamic friction, resulting in a perpendicular orientation of the platelet normal with respect to the flow field. This is why the directions of orientation of the clay platelets are different between the stretching and shearing despite the "common" observation of "an abnormal butterfly pattern". Noteworthy is the fact that, regarding the direction of butterfly patterns, an abnormal butterfly pattern was always observed in the stacking direction of clays, i.e., in the direction of platelet normal, irrespective of the systems, such as NC gels, CNA−polymer solutions, and PEO−laponite solutions.

The retracting behavior observed after stretching suggests the presence of dangling chain. When a NC gel is highly stretched, bridging chains are deformed uniformly between clay platelets. On the other hand, dangling and loop chains recover their unperturbed dimension after stress-relaxation. Hence, a concentration gradient created between clay platelets by deformation generates an osmotic pressure acting to retract the stretched gel. Since the retraction is governed by diffusion of dangling chains and the solvent water, it takes time for the gel to recover its original size. In conclusion, not only entropy elasticity (instant process) but also osmotic retraction (slow process) play a role to recover the original size.

The SANS results on the contrast-matched NC4 suggest that PNIPA chains are also oriented in the stretching direction with the fashion of $\xi_{para} \sim \lambda$. Therefore, the cross-link density of NC gel is much higher and much effective for transmitting applied stress because clay platelets play a "plane" cross-links rather than "point" cross-links in chemically cross-linking with BIS. The high toughness of NC gels is due to this "plane cross-links" with well-aligned orientation of both clay platelets and PNIPA chains.

Conclusion

The structure and deformation mechanism of PNIPA−clay nanocomposite gels (NC gels) were investigated in terms of small-angle neutron scattering. The following facts were disclosed.

(1) The mechanical properties of NC4 are much superior to those of chemical gel cross-linked with BIS. The strength at break being 87.8 kPa (ca. 10 times as high as that of OR3, 9.4 kPa) and the maximum strain ($= (\lambda - 1)_{NC}$) being 1040% (ca. 50 times as high as that of OR3, 21%).

(2) Noncontrast-matched SANS experiments showed an abnormal-butterfly pattern in NC4 by stretching. However, this was assigned to highly oriented clay platelets by stretching with their surface normal parallel to the stretching direction. The orientational correlations between the butterfly pattern and the platelet gels were found to be the same for both the NC and clay−polymer solutions reported in the literature. That is, the direction of the two lobes in the SANS pattern is the same as the stacking direction of the clay platelets.

(3) Contrast-matched SANS experiments allowed us to study deformation mechanism of PNIPA chains in NC gels. An abnormal-butterfly pattern was observed even in the contrast-matched sample. However, it was found that this is due not to an increase in inhomogeneities but to deformed PNIPA chains between platelets by stretching.

(4) PNIPA chains between clay platelets were observed as a blob. The blob was found to deform rather affinely with increasing the stretching ratio up to $\lambda \approx 2$. Further stretching results in viscoelastic deformation without creep behavior.

(5) A slow retraction process to recover the original size was observed. This is due to the presence of dangling chains. The osmotic pressure created by localization of the dangling chains near clay platelets upon stretching may also be a driving force of this retraction.

(6) The extraordinarily good mechanical properties were ascribed to "plane cross-links" with (i) long polymer chains between platelets and (ii) high density of "force-sustainable" polymer chains.

Acknowledgment. This work is partially supported by the Ministry of Education, Science, Sports and Culture, Japan (Grant-in-Aid 16350120). The SANS experiment was performed with the approval of Institute for Solid State Physics, The University of Tokyo (Proposal Nos. 04-006, 05-214), at Japan Atomic Energy Research Institute, Tokai, Japan.

References and Notes

(1) Schmidt, H. In *Mater. Res. Soc.*; Schaefer, D. W., Mark, J. E., Eds.; Pittsburgh, 1990; p 3.
(2) Novak, B. M. *Adv. Mater.* **1993**, *5*, 422.
(3) Lal, J.; Auvray, L. *Mol. Cryst. Liq. Cryst.* **2001**, *356*, 503.
(4) Schmidt, G.; Nakatani, A. I.; Butler, P. D.; Han, C. C. *Macromolecules* **2002**, *35*, 4725.
(5) Lin-Gibson, S.; Schmidt, G.; Han, C. C.; Hobbie, E. K. *J. Chem. Phys.* **2003**, *119*, 8080.
(6) Lin-Gibson, S.; Kim, H.; Schmidt, G.; Han, C. C.; Kobbie, E. K. *J. Colloid Interface Sci.* **2004**, *2004*, 515.
(7) Haraguchi, K.; Takeshita, T. *Adv. Mater.* **2002**, *14*, 1120.
(8) Haraguchi, K.; Takeshita, T.; Fan, S. *Macromolecules* **2002**, *35*, 10162.
(9) Haraguchi, K.; Farnworth, R.; Ohbayashi, A.; Takehisa, T. *Macromolecules* **2003**, *36*, 5732.
(10) Haraguchi, K.; Li, H.-J.; Matsuda, K.; Takehisa, T.; Elliot, E. *Macromolecules* **2005**, *38*, 3482.
(11) Shibayama, M.; Suda, J.; Karino, T.; Okabe, S.; Takehisa, T.; Haraguchi, K. *Macromolecules* **2004**, *37*, 9606.
(12) Saunders, J. M.; Goodwin, J. W.; Richardson, R. M.; Vincent, B. *J. Phys. Chem. B* **1999**, *103*, 9211.
(13) Okabe, S.; Nagao, M.; Karino, T.; Watanabe, S.; Shibayama, M. *J. Appl. Crystallogr.,* in press.
(14) Shibayama, M.; Nagao, M.; Okabe, S.; Karino, T. *J. Phys. Soc. Jpn.* **2005**, *74*, 2728.
(15) Lal, J.; Auvray, L. *J. Appl. Crystallogr.* **2000**, *33*, 673.
(16) Baumgartner, A., Picot, C. E., Eds.; *Molecular Basis of Polymer Networks*; Springer: Berlin, 1989; Vol. 42.

(17) Mendes, E. J.; Lindner, P.; Buzier, M.; Boue, F.; Bastide, J. *Phys. Rev. Lett.* **1991**, *66*, 1595.
(18) Shibayama, M.; Kawakubo, K.; Ikkai, F.; Imai, M. *Macromolecules* **1998**, *31*, 2586.
(19) Rouf, C.; Bastide, J.; Pujol, J. M.; Schosseler, F.; Munch, J. P. *Phys. Rev. Lett.* **1994**, *73*, 830.
(20) Mendes, E.; Oeser, R.; Hayes, C.; Boue, F.; Bastide, J. *Macromolecules* **1996**, *29*, 5574.
(21) Schmidt, G.; Nakatani, A. I.; Butler, P. D.; Karim, A.; Han, C. C. *Macromolecules* **2000**, *33*, 7219.
(22) Karino, T.; Okumura, Y.; Zhao, C.; Kataoka, T.; Ito, K.; Shibayama, M. *Macromolecules* **2005**, *38*, 6161.
(23) Shibayama, M. *Macromol. Chem. Phys.* **1998**, *199*, 1.
(24) Shibayama, M.; Norisuye, T.; Ikkai, F. *J. Phys. Soc. Jpn., Suppl. A* **2001**, *70*, 306.
(25) Shibayama, M.; Norisuye, T.; Nomura, S. *Macromolecules* **1996**, *29*, 8746.
(26) Shibayama, M.; Isaka, Y.; Shiwa, Y. *Macromolecules* **1999**, *32*, 7086.
(27) Malwitz, M. M.; Butler, P. D.; Porcar, L.; Angelette, D. P.; Schmidt, G. *J. Polym. Sci., Part B: Polym. Phys.* **2004**, *42*, 3102.

MA051979H